Integrated metabolomics and transcriptomics analysis of monolayer and neurospheres from glioblastoma cells

Joana Peixoto (jpeixoto@ipatimup.pt)
Universidade do Porto Instituto de Investigacao e Inovacao em Saude https://orcid.org/0000-0001-9469-5680

Sudha Janaki-Raman
Julius-Maximilians-Universitat Wurzburg

Lisa Schlicker
Julius-Maximilians-Universitat Wurzburg

Werner Schmitz
Julius-Maximilians-Universitat Wurzburg

Susanne Walz
Julius-Maximilians-Universitat Wurzburg

Christel Herold-Mende
Heidelberg University

Paula Soares
Universidade do Porto Instituto de Investigacao e Inovacao em Saude

Almut Schulze
Julius-Maximilians-Universitat Wurzburg

Jorge Lima
Universidade do Porto Instituto de Investigacao e Inovacao em Saude

Research

Keywords: glioblastoma, neurospheres, monolayer, metabolome, transcriptome, arginine metabolism

Posted Date: July 21st, 2020

DOI: https://doi.org/10.21203/rs.3.rs-44975/v1

Abstract

Background: Altered metabolism is a hallmark of cancer and metabolic reprogramming can regulate several malignant properties to drive tumourigenesis. Metabolic processes contribute to carcinogenesis by modulating proliferation, survival and differentiation. Here, we studied how metabolic pathways are deregulated in cancer stem-like cells, a specific pool of cells that is thought to be responsible for cancer growth and recurrence. Cancer stem-like cells are particularly relevant in glioblastoma (GBM), the most lethal form of primary brain tumours.

Methods: We have analysed the transcriptome and metabolome of an established GBM cell line (U87) and a patient-derived GBM stem-like cell line (NCH644) exposed to neurosphere or monolayer culture conditions. By integrating transcriptome and metabolome data, we identified key metabolic pathways and gene signatures that are associated with stem-like and differentiated states in GBM cells.

Results: By principal component analysis and hierarchical clustering, we demonstrated that neurospheres and monolayer cells differ substantially in their metabolism and gene regulation. Furthermore, by performing a joint pathway analysis of transcriptome and metabolome data, we found that neurosphere culture conditions induce a similar metabolic rewiring in the two cellular systems and significantly regulate the same metabolic pathways. Finally, arginine biosynthesis was identified as the most significantly regulated pathway in neurospheres from both cell lines, although individual nodes of this pathway were distinctly regulated in the two cellular systems.

Conclusions: Neurosphere conditions, as opposed to monolayer conditions, cause a transcriptomic and metabolic rewiring that may be crucial for the regulation of stem-like features. Arginine biosynthesis may be a key metabolic pathway in stemness regulation, by supporting the specific needs of the different cell populations. Different GBM cell lines show distinct regulation of these metabolic pathways, which are crucial to direct metabolites towards nucleotide or arginine synthesis, respectively. Finally, as part of open science data, the data set generated is of great value as a resource for the scientific community.

Background

The cancer stem cell concept is based on the scientific discovery that tumours, like normal tissues, are composed of subpopulations of cells that can both self-renew and differentiate into several different cell populations. These cells can drive tumour initiation, maintenance and progression, as well as cancer recurrence or metastasis. Specifically in glioblastoma (GBM) models, both *in vitro* and *in vivo* studies have identified the existence of glioblastoma stem-like cells (GSCs) expressing stem cell-related markers, which are able to initiate and recapitulate tumour heterogeneity when injected orthotopically into mice [1, 2]. In this context, GSCs are defined as tumour cells with unlimited self-renewal potential, multipotent differentiation capacity and high tumourigenic ability [1]. Moreover, GSCs have been defined as mediators of therapy resistance by circumventing radio- and chemotherapy and by driving invasion, angiogenesis and recurrence [3–8]. Besides, GSCs can be functionally distinguished from their differentiated tumour

progeny at core levels ranging from transcription and epigenetics to metabolic regulation. The high degree of intratumoral heterogeneity, along with the infiltrative, migratory and plastic nature of GBM cells, as well as the high recurrence rate of this disease, represent the major contributors for the poor prognosis of GBM patients.

The available *in vitro* methods to isolate and/or enrich for GSCs involve using defined suspension cultures to grow and propagate GBM cells, distinguishing them from the non-stem counterparts [9, 10]. This is known as the neurosphere formation assay, which depends on self-renewal properties of GSCs to allow their survival in defined non-adherent conditions. Using primary human GBMs, it was reported that cells propagated *in vitro* under defined culture conditions could form neurospheres enriched for cells exhibiting typical GSC characteristics: potential for indefinite self-renewal and capacity for terminal differentiation into glial and neuronal lineages [2]. Moreover, these cells displayed gene expression profiles and biological behaviour that closely mimic their parental primary tumours, in contrast with tumour cells grown under standard culture conditions. In fact, standard culture conditions were not able to enrich for GSCs, ultimately leading to the propagation of a population of cells that remotely resembled their parental tumours [2].

As a disease that requires building blocks for rapid cell proliferation and survival, cancer is characterized by profound metabolic remodelling that is meant for accumulating metabolic intermediates, which are then used as a source of biomass. However, it has become evident that besides providing energetic and biomass supply, altered metabolic circuits exert effects on shaping cellular tumourigenic properties and fate, ultimately controlling the establishment and maintenance of the tumourigenic state of a cell. Moreover, most studies in the cancer metabolism field have not considered that most tumours contain metabolically distinct cell populations and that this might impose a challenge for metabolism-targeting treatments.

In this study, we have integrated metabolomics and transcriptomics data to disclose key metabolic pathways involved in neurosphere (NS) regulation, as opposed to monolayer (ML) cultures in GBM cells. We unveiled that NS cultures, when compared with ML cultures, were able to cause the downregulation of differentiation-related gene signatures, which supports the use of these culture conditions for GSCs study. By making use of two different cellular systems, an established GBM cell line adapted to grow in ML conditions (U87) and patient-derived stem cells adapted to grow under NS conditions (NCH644), we have provided evidences that NS cultures cause a similar metabolic rewiring in the two cellular systems. Furthermore, arginine biosynthesis, the most significantly regulated pathway in NS was differentially regulated in the two cell lines, revealing that different metabolic fates caused by the expression of specific key players of the pathway can ultimately support the metabolic needs of the two cell lines.

Materials And Methods

Cell culture in monolayer conditions

U87 cells were grown in 10 cm dishes with DMEM high glucose (Sigma 6546 or Biowest L0106) supplemented with 10% FBS (Sigma 7524), 2 mM glutamine (Sigma 59202C or Biowest X0550) and 1% penicillin/streptomycin (Sigma 4333 or Biowest L0022100). NCH644 cells, normally grown under neurosphere conditions (see Sect. 2.2), were transferred to monolayer conditions by singularizing neurospheres with accutase and plating them in 10 cm dishes with DMEM high glucose (Sigma 6546) supplemented with 10% FBS (Sigma 7524), 2 mM glutamine (Sigma 59202C) and 1% penicillin/streptomycin (Sigma 4333). Cells were maintained in a cell incubator at 37 °C, 5% CO2 and a relative humidity of 95%.

Cell culture for neurosphere formation

For neurosphere formation of U87 cell line, 20,000 cells were plated per well in low adhesion 6-well plates coated with poly-HEMA (Poly 2-hydroxyethyl methacrylate; Sigma P3932), with DMEM F12 (Life technologies 21331046 or Biowest 0090) supplemented with 2 mM glutamine (Sigma 59202C or Biowest X0550), 1% penicillin/streptomycin (Sigma 4333 or Biowest L0022100), 20 ng/mL bFGF (Peprotech 100-18B), 20 ng/mL EGF (Peprotech AF-100-15), 10 ng/mL LIF (Peprotech 0300-05) and 1x B27 (Thermo Fisher Scientific 12587010) and maintained in a cell incubator at 37 °C, 5% CO2 and a relative humidity of 95%.

For neurosphere formation of NCH644 cell line, cells were plated in hydrophobic surface T75 flasks (Sarstedt) with DMEM F12 (Life technologies 21331046) supplemented with 2 mM glutamine (Sigma 59202C or Biowest X0550), 1% penicillin/streptomycin (Sigma 4333 or Biowest L0022100), 20 ng/mL bFGF (Biomol 50361.50), 20 ng/mL EGF (Invitrogen PHG0311) and 1x BIT Admixture (Pelo Biotech PB-SH-033-0000) and maintained in a cell incubator at 37 °C, 5% CO2 and a relative humidity of 95%.

RNA sequencing

The experiment was performed in triplicate for each condition. RNA was isolated with the RNeasy Mini Kit with additional DNase I digestion according to manufacturer's protocol (Qiagen). RNA was eluted in 40 µl RNAase free H_2O and kept on ice and concentration was measured using a standard sense chip for Bioanalyzer (Agilent). One µg RNA per each condition was used for library preparation. The library was prepared using the NEBNext Ultra RNA library prep kit for Illumina and the NEBNext Multiplex Oligos for Illumina (Dual Index Primers Set 1), according to the manufacturer's instructions. H_2O was used as negative control to check the purity of the preparation. Amplification by PCR was performed for 12 cycles and the PCR products were purified using the Agencourt AMPure XP beads. The quality of the purified DNA was verified on the Bioanalyzer (Agilent) before performing the sequencing, using the Illumina GAIIx sequencer. All samples were mixed at equimolar concentration of 300 nM.

Base calling was performed with Illumina's CASAVA software and overall sequencing quality was tested using the FastQC script. Reads were aligned to the human genome (hg19) with TopHat2 and Bowtie v0.12.8 using default parameters [11, 12]. Mapped reads per gene (EnsEMBL GRCh37, release 74) were counted using the "summarizeOverlaps" function in the GenomicAlignments R package, non-expressed

genes were removed (mean read count per gene over all samples > 1) and TMM normalized with EdgeR. Gene set enrichment analysis was performed with the C2, C5 and Hallmark collection from the MSigDB v5.2 with default parameters and 1000 permutations [13, 14]. Principle component analysis (PCA) was performed with the prcomp function from R after centring sequencing depth-normalized expression values of all expressed genes (n = 18 457).

Extraction of water-soluble metabolites from cells

For metabolite extraction of monolayer cells, 50,000 U87 cells were plated per well of a 6-well plate and 500,000 NCH644 cells were plated in a 10 cm dish. Cells were washed with cold 154 mM ammonium acetate, snap frozen in liquid nitrogen and scraped off after addition of 0.5 mL ice-cold methanol/water (80/20, v/v) containing 0.25 µM of the internal standard lamivudine (Sigma). For metabolite extraction of neurospheres, 20,000 U87 cells were plated per well of a poly-HEMA coated 6-well plate and 500,000 NCH644 cells were plated in a hydrophobic surface T75 flask. 0.5 mL ice-cold methanol/water (80/20, v/v) containing 0.25 µM of the internal standard lamivudine (Sigma) was added to collected, washed and snap frozen neurospheres. The resulting suspension was transferred to a reaction tube, mixed vigorously and centrifuged (2 minutes, 16 000 g). Supernatants were transferred to a Strata® C18-E column (Phenomenex) which were previously activated with 1 ml of CH_3CN and 1 ml of MeOH/H_2O (80/20, v/v). The eluate was evaporated in a vacuum concentrator. The resulting residue was dissolved in 50 µl 5 mM NH_4OAc in CH_3CN/H_2O (25/75, v/v). The pellets were kept for protein determination.

Liquid chromatography – mass spectrometry (LC-MS)

Samples were diluted 1:2 with CH_3CN and 5 µl of each sample was applied to a HILIC column (Acclaim Mixed-Mode HILIC-1, 3 µm, 2.1*150 mm). Metabolites were separated at 30 °C by LC using a DIONEX Ultimate 3000 UPLC system and the following solvents: Solvent A consisting of 5 mM NH_4OAc in CH_3CN/H_2O (5/95, v/v) and solvent B consisting of 5 mM NH_4OAc in CH_3CN/H_2O (95/5, v/v). The LC gradient program was: 100% solvent B for 1 minute, followed by a linear decrease to 40% solvent B within 5 minutes, then maintaining 40% B for 13 minutes, then returning to 100% B in 1 minute and 5 minutes 100% solvent B for column equilibration before each injection. The flow rate was maintained at 350 µL/min. The eluent was directed to the hESI source of the Q Exactive mass spectrometer (QE-MS) from 1.85 minutes to 18.0 minutes after sample injection (Thermo Scientific, Bremen, Germany). The scan range was set to 69.0 to 1000 m/z with a resolution of 70,000 and polarity switching. Peaks corresponding to the calculated metabolites masses (MIM +/- H + ± 2 mMU) were integrated using TraceFinder software (Thermo Scientific, Bremen, Germany).

Results

Transcriptomic profile of monolayer and neurospheres

To identify significantly regulated genes in GBM neurospheres (NS) versus monolayer (ML) cultures, U87 and NCH644 cells were exposed to ML or NS culture conditions and total RNA was prepared.

Transcriptomics analysis by RNA sequencing identified a total of 18,457 genes across all conditions. Principal component analysis (PCA) revealed a global transcriptomic rewiring when comparing ML with NS in both cell lines (Fig. 1A), which is also shown by hierarchical clustering (Fig. 1B), suggesting that cells exposed to the different culture conditions diverge in their gene expression profile. PC1 accounted for 46% of all variability in U87 cells and nearly 48% in NCH644 cells. In total, 1334 differentially expressed genes were identified in U87 cells and 1229 genes in NCH644 cells with an FDR < 0.05 and a log2FC > ± 1 (Additional file 1 - Tables 1 and 2). U87 and NCH644 NS presented 961 and 510 upregulated genes and 373 and 719 downregulated genes, respectively (Fig. 1C). From these, 124 genes were commonly regulated by both U87 and NCH644 NS cells: 70 commonly upregulated genes and 54 commonly downregulated genes in NS over ML cells (Fig. 1C). Additionally, 115 genes were differentially expressed in NS of the two cell lines: 16 genes were upregulated in NCH644 and downregulated in U87 cells, while 99 genes were upregulated in U87 and downregulated in NCH644 cells (Fig. 1C). Corresponding heat maps and volcano plots are also shown (Fig. 1D and E).

To gain further insight into the processes that are differentially regulated between ML and NS conditions, gene set enrichment analysis (GSEA) was performed using gene sets assigned to crucial biological processes, namely the C2 collection for curated gene sets, C5 for gene ontology gene sets and H for hallmark gene sets (www.gsea-msigdb.org). FDR values were considered to indicate significant enrichment when smaller than 0.25.

GSEA revealed 292 C2 gene sets, 143 C5 gene sets and 21 H gene sets that show significantly higher expression in U87 NS compared to ML (Additional file 1 - Table 3). On the other hand, 238 C2 gene sets, 157 C5 gene sets and 4 H gene sets showed higher expression in ML compared to NS (Additional file 1 - Table 3). Surprisingly, in NCH644 cells, GSEA showed no gene sets that were significantly induced in NS compared to ML, while 50 C2 gene sets, 142 C5 gene sets and 8 H gene sets were found to be upregulated in ML over NS (Additional file 1 - Table 4). From these, gene sets assigned to general traits such as metabolism, proliferation/apoptosis and stem/differentiation processes were selected, and the respective enrichment plots are displayed (Figs. 2 and 3). In U87 cells, a previously defined stem cell signature showed clear enrichment in the NS condition, while ML cells presented an enrichment of glial cell and oligodendrocyte differentiation signatures (Fig. 2A). This strongly suggests that indeed NS culture conditions induce a stem-like phenotype, while ML culture conditions maintain cells under a more differentiated state. Moreover, U87 NS cultures showed an enrichment of an apoptosis gene signature, while several signatures associated with cell cycle, translation and DNA replication/repair were downregulated (Fig. 2B), suggesting that U87 NS have lower proliferative capacity than their ML counterpart. Gene sets representing metabolic pathways, including mitochondrial respiratory chain assembly, tricarboxylic acid (TCA) cycle, pentose phosphate pathway (PPP) and glutamine metabolism were down in U87 NS (Fig. 2C), while a gene set representing negative regulation of nucleotide metabolism was upregulated (Fig. 2C), further supporting a lower proliferation rate and metabolic rewiring driven by altered gene expression. On the contrary, two gene sets associated with hypoxia and regulation of glucose metabolism were upregulated in U87 NS (Fig. 2C), both of which have already been associated with stem-like features in GBM [15–17]. Additionally, a gene set associated with the nitric

oxide pathway was downregulated in U87 NS, pointing at a possible regulation of nitric oxide synthesis in neurospheres (Fig. 2C).

While no gene sets were enriched in NS cultures in NCH644 cells, several gene sets mapping to glial differentiation were upregulated in ML cultures (Fig. 3A), again supporting that this culture condition enriches for cell differentiation. In contrast to U87, which displayed an enrichment of an apoptosis gene signature in NS, NCH644 showed a downregulation of the same gene signature in NS cultures, along with the downregulation of an oxidative stress gene set (Fig. 3B). This suggests that NCH644 cells exposed to NS conditions may not be under the same proliferation inhibition as U87 cells. Altogether, the results indicate that NCH644 cells undergo a less substantial restructuring of their transcriptional activity when exposed to the two culture conditions, as fewer genes sets were found to be regulated, when compared to U87. Nevertheless, both cell lines showed differential expression of gene expression signatures associated with glial differentiation and stemness and thus constitute appropriate models to study different processes under stem and differentiation conditions.

Metabolic profile of monolayer and neurospheres

To analyse general metabolome differences between ML and NS conditions, metabolites were extracted from cells exposed to either culture condition and analysed by LC-MS. We identified a total of 84 metabolites in U87 cells and 99 metabolites in NCH644 cells. PCA clearly separated ML from NS conditions in both cell lines (Fig. 4A), which is also shown by hierarchical clustering of the different samples (Fig. 4B). Specifically, PC1 accounted for nearly 92% of all variability in U87 cells and 98% in NCH644 cells. It is also evident that U87 ML replicates clustered close together, while U87 NS samples were slightly more disperse. In contrast, NCH644 ML replicates are more disperse when compared to their respective NS samples. This can reflect the degree of adaptation of different cell populations to certain culture conditions. U87 is typically an adherent cell line adapted to grow in ML conditions, while NCH644 is a suspension cell line adapted to grow under NS conditions. By changing their respective standard culture conditions, these cells have to adapt to the new environment through potentially driver modifications in their metabolic behaviour, denoted by the different clustering of ML and NS replicates in each cell line. Furthermore, PC1 values show that the different cell culture methods introduce substantial changes in the metabolome, while in the transcriptome, although also heavily affected, the variability between NS and ML were not as strongly defined by PC1 values as in the metabolome.

Statistical analysis of the metabolome data set identified 63 metabolites significantly altered in ML vs. NS from U87 cells and 72 metabolites in ML vs. NS from NCH644 cells (Additional file 1 - Tables 5 and 6). Heat maps and volcano plots for these analyses are shown in Fig. 4C and D. Interestingly, both cells lines presented only a small number of metabolites that were more abundant in NS compared to ML condition (9 in U87 and 7 in NCH644, respectively). In contrast, a large number of metabolites showed significant downregulation in NS compared to ML (54 in U87 and 65 in NCH644) (Fig. 4C, D and E). Out of the downregulated metabolites, 35 were commonly regulated in both cell lines, while only one metabolite – hypoxanthine – was more abundant in NS compared to ML in both cell lines (Fig. 4E). These results indicate that NS conditions cause a metabolic rewiring towards reduced metabolite availability which

points to a lower cellular metabolic activity. Additionally, three metabolites were regulated contradictorily in the two cell lines: U87 NS presented significantly higher levels of arginine, guanine and guanosine, in comparison with ML cells, while NCH644 NS had significantly lower levels of the same metabolites (Fig. 4E).

To identify specific metabolic pathways regulated by the different culture conditions, we used the metabolome data to perform a pathway analysis in MetaboAnalyst and selected metabolic pathways with an FDR < 0.05 and a pathway impact above 0.5 (Additional file 1 - Tables 7 and 8). This analysis showed that four metabolic pathways were commonly regulated in both U87 and NCH644 ML vs. NS cells. These were: “Arginine biosynthesis”, “Alanine, aspartate and glutamate metabolism”, “Citrate cycle (TCA cycle)” and “Pyrimidine metabolism” (Fig. 4F). Additionally, the pathways “Purine metabolism”, “D-glutamine and D-glutamate metabolism”, “Glutathione metabolism” and “Glycine, serine and threonine metabolism” were uniquely regulated in NCH644 ML vs. NS cells (Fig. 4F). This may suggest that commonly regulated pathways could be responsible for the induction and/or maintenance of the NS phenotype. On the other hand, uniquely regulated pathways may explain specific cell line features that may not reflect general NS traits.

Joint metabolomics and gene expression pathway analysis of monolayer and neurospheres

To define the most relevant metabolic pathways regulated in NS over ML cells, a joint pathway analysis was performed in MetaboAnalyst by combining metabolomics and gene expression data. Only significantly altered genes and metabolites were considered for this analysis (FDR < 0.05). Again, metabolic pathways with an FDR lower than 0.05 and a pathway impact above 0.5 were selected for further consideration (Additional file 1 - Tables 9 and 10). Three common pathways were found to be regulated in both U87 and NCH644 ML vs. NS cells: “Arginine biosynthesis”, “Alanine, aspartate and glutamate metabolism” and “Glutathione metabolism” (Fig. 5A). Furthermore, NCH644 ML vs. NS cells presented additional uniquely regulated pathways: “Purine metabolism” and “Histidine metabolism”. Since arginine metabolism was the most significantly regulated pathway in both cell lines, we analysed the individual components within this metabolic pathway in more detail. By evaluating the expression of significantly regulated genes involved in arginine biosynthesis, we found that U87 NS present a strong upregulation of argininosuccinate synthase (ASS1) (log2FC = 4.65), while NCH644 NS displayed a strong downregulation of this gene (log2FC = -3.16) (Fig. 5B). ASS1 catalyses the rate-limiting step for arginine biosynthesis in the urea cycle by combining two amino acids, citrulline and aspartate, to form argininosuccinate (Fig. 5C). We therefore evaluated the expression of other enzymes and metabolites involved in urea cycle metabolism in both cell lines. We observed that multiple urea cycle components were significantly altered between NS and ML cultures in the two cell lines (Fig. 5D and E). In particular, U87 NS showed an upregulation of the genes coding for arginine decarboxylase (ADC) (log2FC = 1.68), solute carrier family 1 member 3 (SLC1A3) (log2FC = 1.86), arginase 2 (ARG2) (log2FC = 1.27) and N-acetylglutamate synthase (NAGS) (log2FC = 1.07), while a downregulation of ornithine decarboxylase 1 (ODC1) (log2FC = -0.24) and solute carrier family 25 member 15 (SLC25A15) (log2FC = -0.88) was

observed (Fig. 5D). Concomitantly, U87 NS presented significantly higher levels of arginine (log2FC = 1.08), and lower levels of carbamoylaspartate (log2FC = -5.33), proline (log2FC = -0.73), ornithine (log2FC = -1.17), citrulline (log2FC = -6.25) and aspartate (log2FC = -1.11) (Fig. 5E). These results point towards an active urea cycle metabolism, with the usage of aspartate to fuel arginine synthesis (Fig. 6A). In contrast, NCH644 NS presented an upregulation of the genes coding for ornithine aminotransferase (OAT) (log2FC = 0.62), ODC1 (log2FC = 0.19), SLC25A15 (log2FC = 1.05) and SLC1A3 (log2FC = 0.56), with downregulation of carbamoyl-phosphate synthase 1 (CPS1) (log2FC = -0.72), nitric oxide synthase 1 (NOS1) (log2FC = -0.37) and solute carrier family 25 member 13 (SLC25A13) (log2FC = -0.30) (Fig. 5D). Additionally, NCH644 NS presented significantly lower levels of arginine (log2FC = -2.21), ornithine (log2FC = -5.86), aspartate (log2FC = -2.95), citrulline (log2FC = -5.88) and proline (log2FC = -1.36) (Fig. 5E).

Taken together, these results suggest that although the same metabolic pathway is significantly regulated in both U87 and NCH644 NS, the metabolites and enzymes involved in the pathway can be differentially regulated to achieve different metabolic needs. U87 cells exposed to NS condition show a clear downregulation of proliferation, thereby reducing their demand for nucleotide biosynthesis. They upregulate ASS1 to direct aspartate into the urea cycle for arginine biosynthesis (Fig. 6A). In contrast, NCH644 cells exposed to NS conditions, where they continue to proliferate, may downregulate ASS1 to prevent the incorporation of aspartate into the urea cycle. Instead, aspartate is shuttled away from arginine biosynthesis towards nucleotide synthesis to maintain proliferation (Fig. 6B).

Discussion

It is widely recognised that defined culture conditions enabling the formation of neurospheres lead to an enrichment of stem-like properties of these cells, which can be functionally distinguished from their differentiated counterpart at many levels ranging from genetic expression to metabolic regulation. Our results support this notion by showing that changes in culture conditions from adherent ML to suspension NS cause a global rewiring of the transcriptome and metabolome, with a high degree of separation shown by PCA and hierarchical clustering. Although U87 cells are adapted to grow under ML conditions, it is evident that their NS cultures are capable of triggering a more stem-like phenotype, by inducing the upregulation of a stem cell-related gene set and the downregulation of differentiation-related gene sets. Similarly, NCH644 cells, which are adapted to grow under NS conditions, also showed downregulation of the same differentiation-related gene sets, supporting that culture conditions may dictate the more stem or differentiated state of cells, respectively. Thus, both U87 and NCH644 are appropriate cellular systems to study stem and differentiated states in GBM, by challenging cells with defined culture conditions.

Since the main purpose of this work was to study metabolic similarities and differences between U87 and NCH644 cells under ML vs. NS conditions, the approach was to perform a general metabolic profiling using LC-MS metabolomics followed by detailed pathway analysis using the MetaboAnalyst platform and a Joint Pathway analysis, which integrates metabolomics and gene expression data. General

metabolome analysis revealed that, from the 36 metabolites that were equally regulated in both U87 and NCH644 cells, 35 were found to be downregulated in NS compared to ML. These included TCA cycle metabolites (citrate, α-ketoglutarate, succinate, fumarate and malate), amino acids (alanine, aspartate, isoleucine, citrulline, glutamate, histidine, methionine, ornithine, phenylalanine, proline, sarcosine, serine, threonine and tyrosine) and purine/pyrimidine metabolism-related metabolites (xanthine, xanthosine, UDP, thymidine and thymine), suggesting that NS of both U87 and NCH644 NS may be exhibiting reduced overall cellular metabolic activity, compared to their ML counterparts. On the other hand, hypoxanthine was the only metabolite presenting higher levels in both U87 and NCH644 NS, which points out a possible role of this metabolite in stem-like cells. Hypoxanthine is converted into inosine monophosphate (IMP) by the enzyme hypoxanthine guanine phosphoribosyltransferase (HPRT), which plays a major role in the salvage pathway for purine biosynthesis. Thus, hypoxanthine accumulation could be indicative of an impaired salvage pathway and a consequent increase in the *de novo* purine synthesis as a compensatory mechanism. In fact, despite the existence of two different pathways for purine synthesis – *de novo* and salvage pathways – cancer cells tend to display a high rate of the *de novo* nucleotide synthesis [18, 19]. U87 NS presented significantly higher levels of guanine and guanosine, possibly due to this increase in the *de novo* purine synthesis. However, NCH644 NS presented significantly lower levels of guanine and guanosine, suggesting that in these cells, these metabolites are either being less produced or rapidly metabolized. The HPRT enzyme may be using guanine for guanine monophosphate (GMP) production in NCH644 NS, instead of using hypoxanthine for IMP synthesis in the salvage pathway. Since the salvage pathway recycles components of existing nucleotides and skips energetically expensive steps of *de novo* nucleotide biosynthesis [20], the production of purines via the salvage pathway in NCH644 NS may be more energy efficient in comparison to U87 NS. This may also support the high proliferative state of NCH644 NS and prevent the induction of stress and apoptosis. However, since these results only represent a snapshot of the metabolic pathways that are active in the cells, decrease in guanine and guanosine levels in NCH644 NS could also be indicative of higher demands for nucleotides for rapid proliferation. Nevertheless, both hypotheses are in line with the gene signatures found to be significantly regulated in U87 NS, which pointed towards reduced proliferation in NS compared to ML condition, which was not observed in NCH644 NS. In fact, although the general metabolome analysis pointed towards a global decrease in metabolic activity of both U87 and NCH644 NS, only U87 cells displayed several altered gene sets indicating reduced proliferation. Gene sets related to proliferation (cell cycle, translation, DNA synthesis and repair) and metabolism (TCA cycle, mitochondrial activity, PPP and glutamine metabolism) were all downregulated in U87 NS, while an apoptosis gene set and a gene signature assigned for a negative regulation of nucleotide metabolism were upregulated, all supporting a lower cellular activity. Contrarily, NCH644 NS presented downregulation of an apoptosis and oxidative stress gene sets, suggesting that ML cells may be facing slower proliferation in contrast with NS in this cell line. Again, adaptation to certain culture conditions may explain why U87 cells, which are not adapted to grow in NS, and NHC644 cells, which are not adapted to grow under ML conditions, may proliferate slower when challenged with different culture conditions.

Noteworthy, metabolic adaptations triggered by NS conditions did not differ substantially between the two cell lines. Actually, both Metaboanalyst analyses using only metabolites or metabolites and genes together, identified similar metabolic pathways regulated in U87 and NCH644 NS cells. In particular, “Arginine biosynthesis” was the most significantly regulated pathway in both cell lines. While this suggests that arginine biosynthesis constitutes a key metabolic pathway in the stimulation and maintenance of the stem-like phenotype, there were clear differences in the regulation of specific components of this pathway between the two cell lines. Indeed, the significant upregulation of *ASS1* in U87 NS and the downregulation of the same gene in NCH644 NS was identified as a major difference that could determine differences in the metabolic fate of aspartate in the two cellular systems.

Aspartate can be used for the synthesis of arginine as part of the cytoplasmic arm of the urea cycle. Through the ATP-dependent activity of ASS1, aspartate is condensed with citrulline to form argininosuccinate and subsequently cleaved into arginine and fumarate by argininosuccinate lyase (ASL). Aspartate can either be synthesized from the TCA cycle metabolite oxaloacetate and then transported to the cytoplasm by the mitochondrial SLC25A13 transporter or taken up by the cells through the SLC1A3 transporter. Since aspartate is also an essential precursor for nucleotide synthesis, conversion of aspartate to argininosuccinate by ASS1 can prevent this metabolite to enter nucleotide biosynthesis, possibly resulting in reduced proliferation. ASS1 upregulation has been reported in ovarian, colorectal, gastric and lung cancers, compared to the corresponding normal tissues [21–24]. While the role of ASS1 in cancer as well as the molecular mechanism mediating ASS1 upregulation remains unclear, it has been described that high ASS1 expression is associated with increased proliferation and tumourigenicity of colorectal cancer [25]. On the other hand, it has been reported that downregulation of urea cycle metabolism, specifically decreased activity of *ASS1* expression, diverts aspartate towards pyrimidine biosynthesis to support cell proliferation, while evading arginine biosynthesis, as part of metabolic reprograming in cancer [26, 27]. Reduced ASS1 expression in cancer is accompanied by increased aspartate metabolism through the trifunctional protein CAD (Carbamoyl-Phosphate Synthetase 2, Aspartate Transcarbamylase and Dihydroorotase), leading to increased pyrimidine synthesis [27]. Importantly, decreased ASS1 expression or arginine depletion in gastric cancer is described to inhibit cancer cell migration and motility, therefore affecting metastasis formation *in vivo* [24].

Besides ASS1, the urea cycle consists of four other main catalytic enzymes: two cytosolic enzymes, ASL and ARG, and two mitochondrial enzymes, CPS1 and ornithine transcarbamylase (OTC) [28]. These enzymes catalyse the synthesis of arginine, ornithine and citrulline, respectively, and the urea cycle not only plays a role in the removal of excess amino-groups but also produces metabolic intermediates for the synthesis of metabolites that are essential for cell survival and proliferation [29, 30]. Additionally, NAGS and the two amino acid transporters – SLC25A13 or citrin and SLC25A15 or ORNT1 (mitochondrial ornithine transporter 1) – also participate in urea metabolism [28].

Among the urea cycle metabolites, we found that both U87 and NCH644 NS presented significantly lower levels of aspartate in comparison with their ML counterpart. Additionally, expression of the high-affinity amino acid transporter SLC1A3 that mediates the uptake of glutamate and aspartate by cells, was

significantly increased in both U87 and NCH644 NS, although much stronger in U87 cells. Since *ASS1* was differentially regulated in the two cell lines, this may suggest that although aspartate is synthesised/taken up by NS cells, its metabolic fate may be very different between the two cell lines. While in U87 NS, aspartate may be shuttled towards arginine synthesis in the urea cycle, NS of NCH644 cells could use aspartate mainly for nucleotide synthesis. In fact, although ASL expression was not significantly changed between ML and NS in both cell lines, arginine levels were significantly increased in U87 NS compared to ML, while being significantly decreased in NCH644 NS. This suggests that U87 cells increase arginine synthesis via the urea cycle when placed in NS conditions while this is not taking place in NCH644 cells. Additionally, ARG2 was significantly increased in U87 NS, along with ADC, an enzyme that catabolizes arginine into agmatine, suggesting that arginine could be further metabolized by these two enzymes for ornithine and agmatine production, respectively. In contrast, the same enzymes were not changed in NCH644 cells. OAT and ODC expression was significantly increased in NCH644 NS, while not being regulated in U87 NS. OAT and ODC are involved in proline and polyamines biosynthesis, respectively, by metabolizing the urea cycle intermediate ornithine. This could suggest that while ornithine in U87 NS is diverted to citrulline to fuel the high demand for arginine through ASS1, ornithine is being diverted in NCH644 NS towards proline and polyamine synthesis. Indeed, the very low levels of ornithine present in NCH644 NS also indicate a diminished arginine metabolism in these cells. Interestingly, the SLC25A15 transporter, which transports ornithine from the cytoplasm to the mitochondria, was found to be significantly upregulated in NCH644 NS, suggesting that the low amount of ornithine in NCH644 NS may be directed to the mitochondria and away from arginine biosynthesis. Although U87 NS also display significantly reduced levels of ornithine, this reduction was not as strong as in NCH644 NS, possibly due to the high expression of ARG2 and NAGS, which maintain an influx of ornithine into the urea cycle for arginine biosynthesis. NAGS catalyses the production of N-acetylglutamate (NAG) from glutamate and acetyl-CoA, which is then used for the production of ornithine, or as an allosteric cofactor for CPS1. Again, supporting the notion that NCH644 NS rewire their metabolism to lower the production of ornithine to feed arginine biosynthesis, CPS1 in these cells was significantly reduced. Finally, NOS1, which produces nitric oxide and citrulline from arginine, was downregulated in NCH644 NS, again pointing to a low arginine catabolism in these cells. In U87 NS, although not presenting significant regulation of the *NOS1* gene itself, a significant downregulation of a gene set assigned to NOS1 metabolism was found, indicating alterations in nitric oxide signalling. However, upregulation of ARG2 and ADC indicates a higher catabolism of arginine in the urea cycle and for agmatine production in these cells.

Together, our results identify arginine metabolism as a key metabolic process associated with stemness in two different cellular systems. While altered arginine metabolism is clearly associated with culture conditions that enrich for stem-like cells, the exact metabolic rewiring or arginine metabolism is distinct between the two cell lines to fulfil cell line specific demands. Thus, the use of different metabolic routes within this pathway ensures cell survival by accomplishing the metabolic needs of each cell system through transcriptional and metabolic adaptations.

Conclusions

Using two different culture conditions in two GBM cell lines, we have shown here that the induction and maintenance of a more stem-like phenotype relies on the remodelling of specific metabolic pathways, and that such a metabolic portrait is fundamentally different from that of cells in a more differentiated state. Importantly, the two cell lines adapted to the different culture conditions in a similar manner and displayed overlapping metabolic behaviour. However, the regulation of the same specific pathway in both cell lines was shown to yield different metabolic outcomes, in order to accomplish specific metabolic demands necessary for their respective growth and survival. Overall, U87 cells responded to growth conditions favouring a stem-like state with *ASS1* upregulation and significantly elevated levels of arginine along with the downregulation of gene signatures associated with cell cycle progression, DNA synthesis and PPP activity. This supports the notion that these cells have a reduced demand of aspartate as a precursor for nucleotide biosynthesis and instead shuttle this metabolite towards arginine generation and the urea cycle. Further work is needed to investigate whether arginine plays a specific role in supporting the stem-like state in these cells. In contrast, NCH644 cultures enriched for stem-like cells showed a substantial downregulation of *ASS1* and significantly lower levels of arginine. Compared to their more differentiated counterparts, these cells did not downregulate gene signatures associated with DNA synthesis, cell cycle and proliferation, indicating that this cell line maintains higher proliferative potential under neurosphere culture conditions. This suggest that these cells direct a higher proportion of aspartate towards nucleotide biosynthesis and have a lower dependence on arginine synthesis. Further experiments using stable isotope labelling are required to determine the exact fate of specific metabolites in the two cellular systems, determine how arginine metabolism is connected to the stem-like state and disclose the complete metabolic rewiring in GBM stem-like cells.

Abbreviations

ADC - arginine decarboxylase

ARG – arginase

ASL - argininosuccinate lyase

ASS1 - argininosuccinate synthase

CAD - carbamoyl-phosphate synthetase 2, aspartate transcarbamylase and dihydroorotase

CPS1 - carbamoyl-phosphate synthase 1

GBM – glioblastoma

GMP- guanine monophosphate

GSC - glioblastoma stem-like cell

GSEA - gene set enrichment analysis

HPRT - hypoxanthine guanine phosphoribosyltransferase

IMP - inosine monophosphate

LC-MS - liquid chromatography – mass spectrometry

ML – monolayer

NAG - N-acetylglutamate

NAGS - N-acetylglutamate synthase

NOS1 - nitric oxide synthase 1

NS – neurosphere

OAT - ornithine aminotransferase

ODC1 - ornithine decarboxylase 1

OTC - ornithine transcarbamylase

PCA - principle component analysis

PPP - pentose phosphate pathway

SLC1A3 - solute carrier family 1 member 3

SLC25A13 - solute carrier family 25 member 13

SLC25A15 - solute carrier family 25 member 15

TCA - tricarboxylic acid

Declarations

Ethics approval and consent to participate

Not applicable

Consent for publication

Not applicable

Availability of data and materials

All data generated or analysed during this study are included in this published article and its supplementary information files.

Competing interests

The authors declare that they have no competing interests

Funding

This work was funded by the European Regional Development Fund (ERDF) through the Operational Programme for Competitiveness and Internationalisation - COMPETE 2020, and Portuguese national funds via FCT – Fundação para a Ciência e a Tecnologia, under the project POCI-01-0145-FEDER-016390:CANCEL STEM. J.P. is financed through a grant from Fundação para a Ciência e a Tecnologia (SFRH/BD/105694/2015). I3S is an Associated Laboratory of the Portuguese Ministry of Science, Technology and Higher Education that is partially supported by Fundação para a Ciência e a Tecnologia.

Authors' contributions

JP performed the experiments, interpreted the data generated and was a major contributor in writing the manuscript. SJ and LS analysed and interpreted the data generated and participated in manuscript revision and editing. WS performed LC/MS running. SW performed RNAseq and GSEA analysis. CH provided resources. PS provided supervision and resources. AS and JL participated in the conceptualization and administration of the project, provided supervision and were major contributors in manuscript revision and editing. All authors read and approved the final manuscript.

Acknowledgements

Not applicable

References

1. Singh SK, Hawkins C, Clarke ID, Squire JA, Bayani J, Hide T, Henkelman RM, Cusimano MD, Dirks PB. Identification of human brain tumour initiating cells. Nature. 2004;432(7015):396–401.
2. Lee J, Kotliarova S, Kotliarov Y, Li A, Su Q, Donin NM, Pastorino S, Purow BW, Christopher N, Zhang W, Park JK, Fine HA. Tumor stem cells derived from glioblastomas cultured in bFGF and EGF more closely mirror the phenotype and genotype of primary tumors than do serum-cultured cell lines. Cancer Cell. 2006;9(5):391–403.
3. Bao S, Wu Q, McLendon RE, Hao Y, Shi Q, Hjelmeland AB, Dewhirst MW, Bigner DD, Rich JN. Glioma stem cells promote radioresistance by preferential activation of the DNA damage response. Nature.

2006;444(7120):756–60.

4. Liu G, Yuan X, Zeng Z, Tunici P, Ng H, Abdulkadir IR, Lu L, Irvin D, Black KL, Yu JS. Analysis of gene expression and chemoresistance of CD133 + cancer stem cells in glioblastoma. Mol Cancer. 2006;5:67.
5. Chen J, Li Y, Yu TS, McKay RM, Burns DK, Kernie SG, Parada LF. A restricted cell population propagates glioblastoma growth after chemotherapy. Nature. 2012;488(7412):522–6.
6. Bao S, Wu Q, Sathornsumetee S, Hao Y, Li Z, Hjelmeland AB, Shi Q, McLendon RE, Bigner DD, Rich JN. Stem cell-like glioma cells promote tumor angiogenesis through vascular endothelial growth factor. Cancer Res. 2006;66(16):7843–8.
7. Cheng L, Huang Z, Zhou W, Wu Q, Donnola S, Liu JK, Fang X, Sloan AE, Mao Y, Lathia JD, Min W, McLendon RE, Rich JN, Bao S. Glioblastoma stem cells generate vascular pericytes to support vessel function and tumor growth. Cell. 2013;153(1):139–52.
8. Wakimoto H, Kesari S, Farrell CJ, Curry WT Jr, Zaupa C, Aghi M, Kuroda T, Stemmer-Rachamimov A, Shah K, Liu TC, Jeyaretna DS, Debasitis J, Pruszak J, Martuza RL, Rabkin SD. Human glioblastoma-derived cancer stem cells: establishment of invasive glioma models and treatment with oncolytic herpes simplex virus vectors. Cancer Res. 2009;69(8):3472–81.
9. Pardal R, Clarke MF, Morrison SJ. Applying the principles of stem-cell biology to cancer. Nat Rev Cancer. 2003;3(12):895–902.
10. Reya T, Morrison SJ, Clarke MF, Weissman IL. Stem cells, cancer, and cancer stem cells. Nature. 2001;414(6859):105–11.
11. Kim D, Pertea G, Trapnell C, Pimentel H, Kelley R, Salzberg SL. TopHat2: accurate alignment of transcriptomes in the presence of insertions, deletions and gene fusions. Genome Biol. 2013;14(4):R36.
12. Langmead B. Aligning short sequencing reads with Bowtie. Curr Protoc Bioinformatics. 2010; Chap. 11 Unit 11 7.
13. Liberzon A, Subramanian A, Pinchback R, Thorvaldsdottir H, Tamayo P, Mesirov JP. Molecular signatures database (MSigDB) 3.0. Bioinformatics. 2011;27(12):1739–40.
14. Subramanian A, Tamayo P, Mootha VK, Mukherjee S, Ebert BL, Gillette MA, Paulovich A, Pomeroy SL, Golub TR, Lander ES, Mesirov JP. Gene set enrichment analysis: a knowledge-based approach for interpreting genome-wide expression profiles. Proc Natl Acad Sci U S A. 2005;102(43):15545–50.
15. Li Z, Bao S, Wu Q, Wang H, Eyler C, Sathornsumetee S, Shi Q, Cao Y, Lathia J, McLendon RE, Hjelmeland AB, Rich JN. Hypoxia-inducible factors regulate tumorigenic capacity of glioma stem cells. Cancer Cell. 2009;15(6):501–13.
16. Soeda A, Park M, Lee D, Mintz A, Androutsellis-Theotokis A, McKay RD, Engh J, Iwama T, Kunisada T, Kassam AB, Pollack IF, Park DM. Hypoxia promotes expansion of the CD133-positive glioma stem cells through activation of HIF-1alpha. Oncogene. 2009;28(45):3949–59.
17. Zhou Y, Zhou Y, Shingu T, Feng L, Chen Z, Ogasawara M, Keating MJ, Kondo S, Huang P. Metabolic alterations in highly tumorigenic glioblastoma cells: preference for hypoxia and high dependency on

glycolysis. J Biol Chem. 2011;286(37):32843–53.
18. Lane AN, Fan TW. Regulation of mammalian nucleotide metabolism and biosynthesis. Nucleic Acids Res. 2015;43(4):2466–85.
19. Tong X, Zhao F, Thompson CB. The molecular determinants of de novo nucleotide biosynthesis in cancer cells. Curr Opin Genet Dev. 2009;19(1):32–7.
20. Becerra A, Lazcano A. The role of gene duplication in the evolution of purine nucleotide salvage pathways. Orig Life Evol Biosph. 1998; 28 (4–6): 539 – 53.
21. Szlosarek PW, Grimshaw MJ, Wilbanks GD, Hagemann T, Wilson JL, Burke F, Stamp G, Balkwill FR. Aberrant regulation of argininosuccinate synthetase by TNF-alpha in human epithelial ovarian cancer. Int J Cancer. 2007;121(1):6–11.
22. Wu MS, Lin YS, Chang YT, Shun CT, Lin MT, Lin JT. Gene expression profiling of gastric cancer by microarray combined with laser capture microdissection. World J Gastroenterol. 2005;11(47):7405–12.
23. Delage B, Fennell DA, Nicholson L, McNeish I, Lemoine NR, Crook T, Szlosarek PW. Arginine deprivation and argininosuccinate synthetase expression in the treatment of cancer. Int J Cancer. 2010;126(12):2762–72.
24. Shan YS, Hsu HP, Lai MD, Yen MC, Chen WC, Fang JH, Weng TY, Chen YL. Argininosuccinate synthetase 1 suppression and arginine restriction inhibit cell migration in gastric cancer cell lines. Sci Rep. 2015;5:9783.
25. Bateman LA, Ku WM, Heslin MJ, Contreras CM, Skibola CF, Nomura DK. Argininosuccinate Synthase 1 is a Metabolic Regulator of Colorectal Cancer Pathogenicity. ACS Chem Biol. 2017;12(4):905–11.
26. Gaude E, Frezza C. Tissue-specific and convergent metabolic transformation of cancer correlates with metastatic potential and patient survival. Nat Commun. 2016;7:13041.
27. Rabinovich S, Adler L, Yizhak K, Sarver A, Silberman A, Agron S, Stettner N, Sun Q, Brandis A, Helbling D, Korman S, Itzkovitz S, Dimmock D, Ulitsky I, Nagamani SC, Ruppin E, Erez A. Diversion of aspartate in ASS1-deficient tumours fosters de novo pyrimidine synthesis. Nature. 2015;527(7578):379–83.
28. Keshet R, Szlosarek P, Carracedo A, Erez A. Rewiring urea cycle metabolism in cancer to support anabolism. Nat Rev Cancer. 2018;18(10):634–45.
29. Erez A, Nagamani SC, Lee B. Argininosuccinate lyase deficiency-argininosuccinic aciduria and beyond. Am J Med Genet C Semin Med Genet. 2011;157C(1):45–53.
30. Husson A, Brasse-Lagnel C, Fairand A, Renouf S, Lavoinne A. Argininosuccinate synthetase from the urea cycle to the citrulline-NO cycle. Eur J Biochem. 2003;270(9):1887–99.

Figures

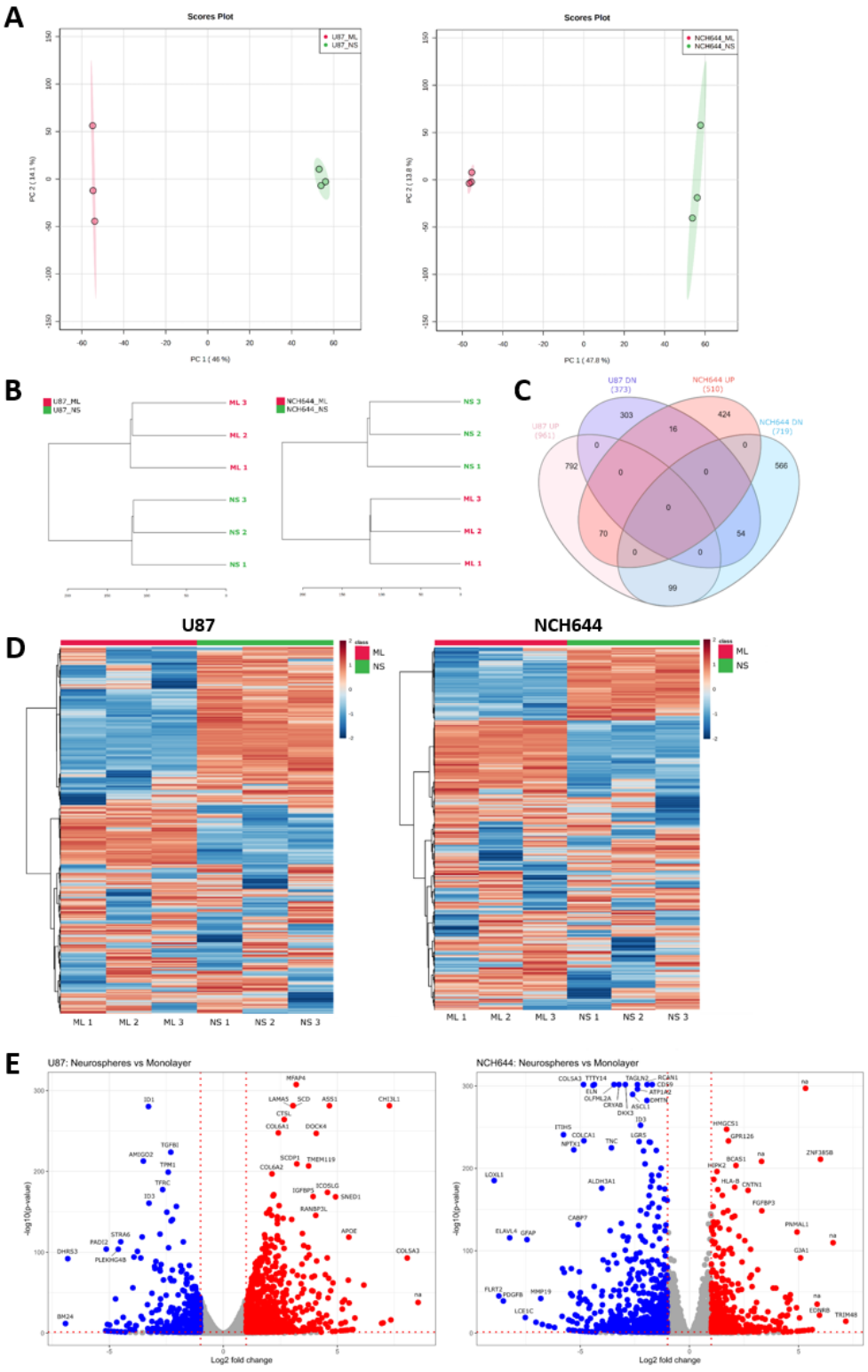

Figure 1

Transcriptomics analysis of ML and NS from U87 and NCH644 cells. A) Principal component analysis and B) Hierarchical clustering of all genes, showing a clear separation between ML and NS samples in both cell lines. C) Venn diagram depicting the number of significantly upregulated and downregulated genes in NS vs ML, as well as the number of commonly and differentially regulated genes between U87

and NCH644 cells (FDR<0.05, log2FC>±1). D) Heatmaps and E) Volcano plots of upregulated (red) and downregulated (blue) genes in NS vs ML from U87 and NCH644 cells (FDR<0.05, log2FC>±1). n=3

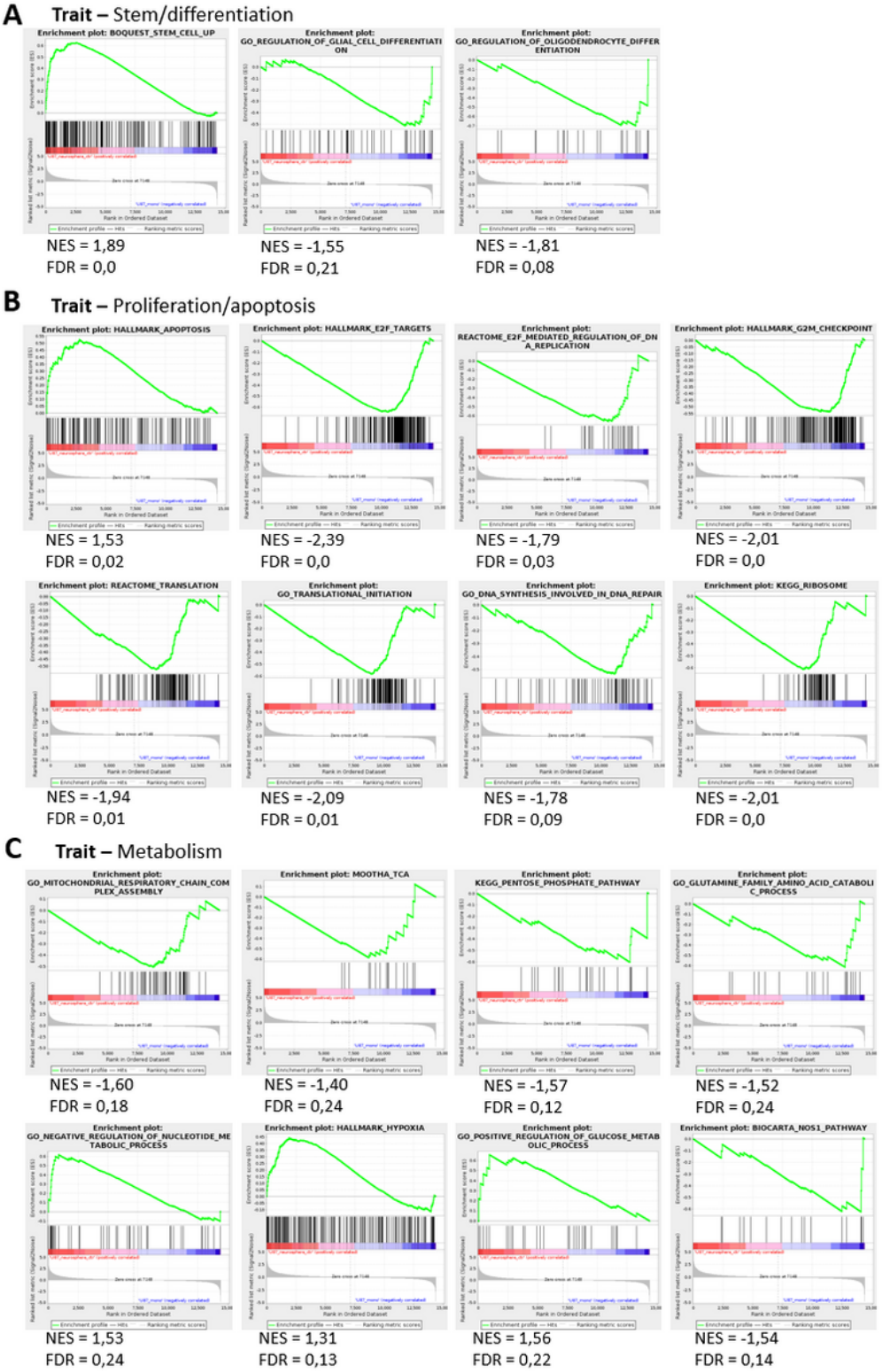

Figure 2

GSEA of gene sets associated with stem/differentiation, proliferation/apoptosis and metabolism traits in NS vs ML from U87 cells. A) A stem cell-associated gene set is upregulated in NS, while two differentiation gene sets are enriched in ML B) An apoptosis gene set is enriched, while several

proliferation-associated gene sets are downregulated in NS. C) Metabolism-associated gene sets, namely mitochondrial respiratory chain assembly, TCA cycle, PPP and glutamine metabolism are downregulated in NS, while a gene set representing negative regulation of nucleotide metabolism is upregulated. Hypoxia and glucose metabolism gene sets are upregulated, while a nitric oxide pathway gene set is downregulated in NS. n=3, FDR<0.25

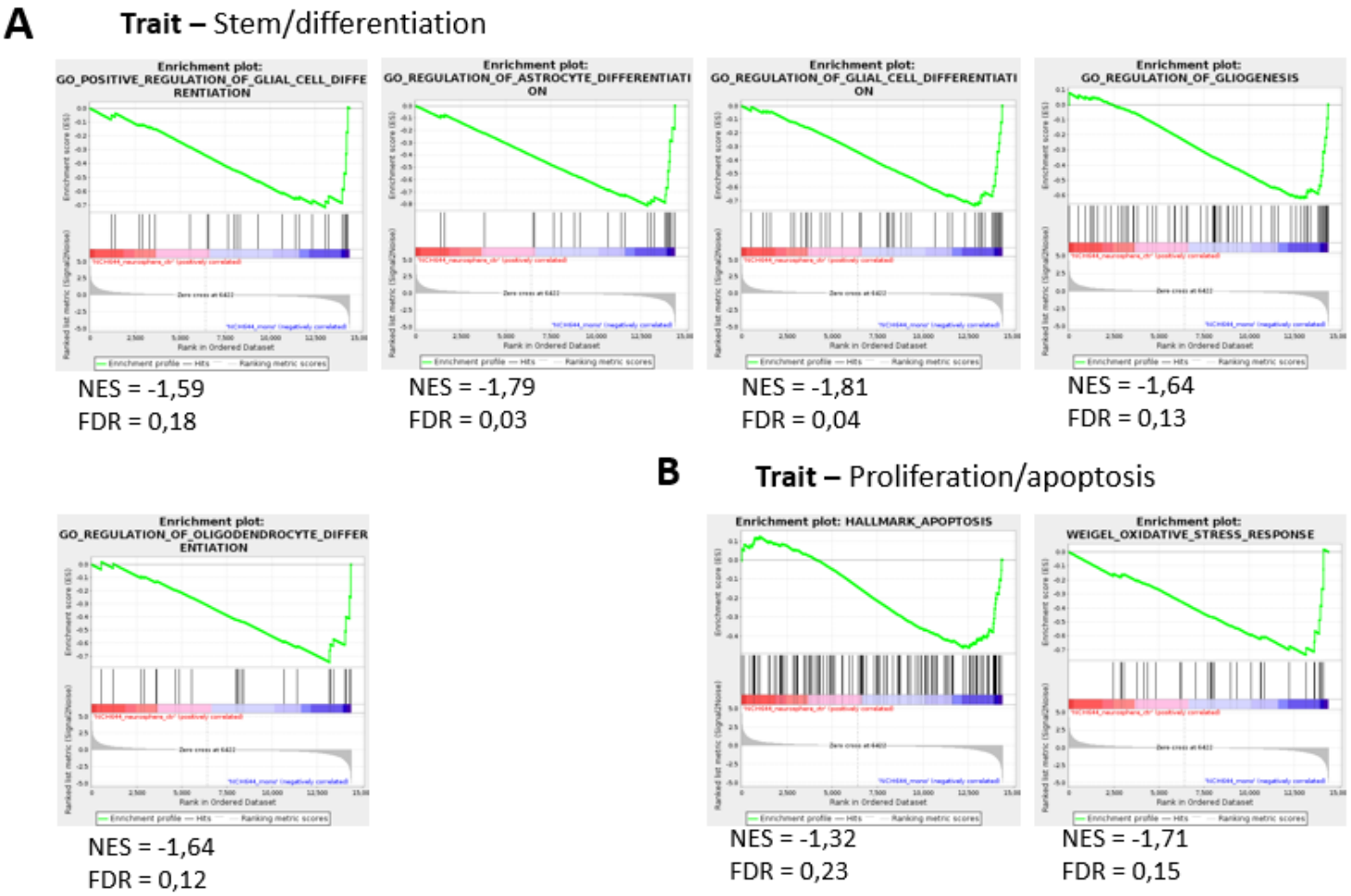

Figure 3

GSEA of gene sets associated with stem/differentiation and proliferation/apoptosis traits in NS vs ML from NCH644 cells. A) Several differentiation-associated gene sets are enriched in NS. B) Gene sets associated with apoptosis and oxidative stress response are downregulated in NS. n=3, FDR<0.25

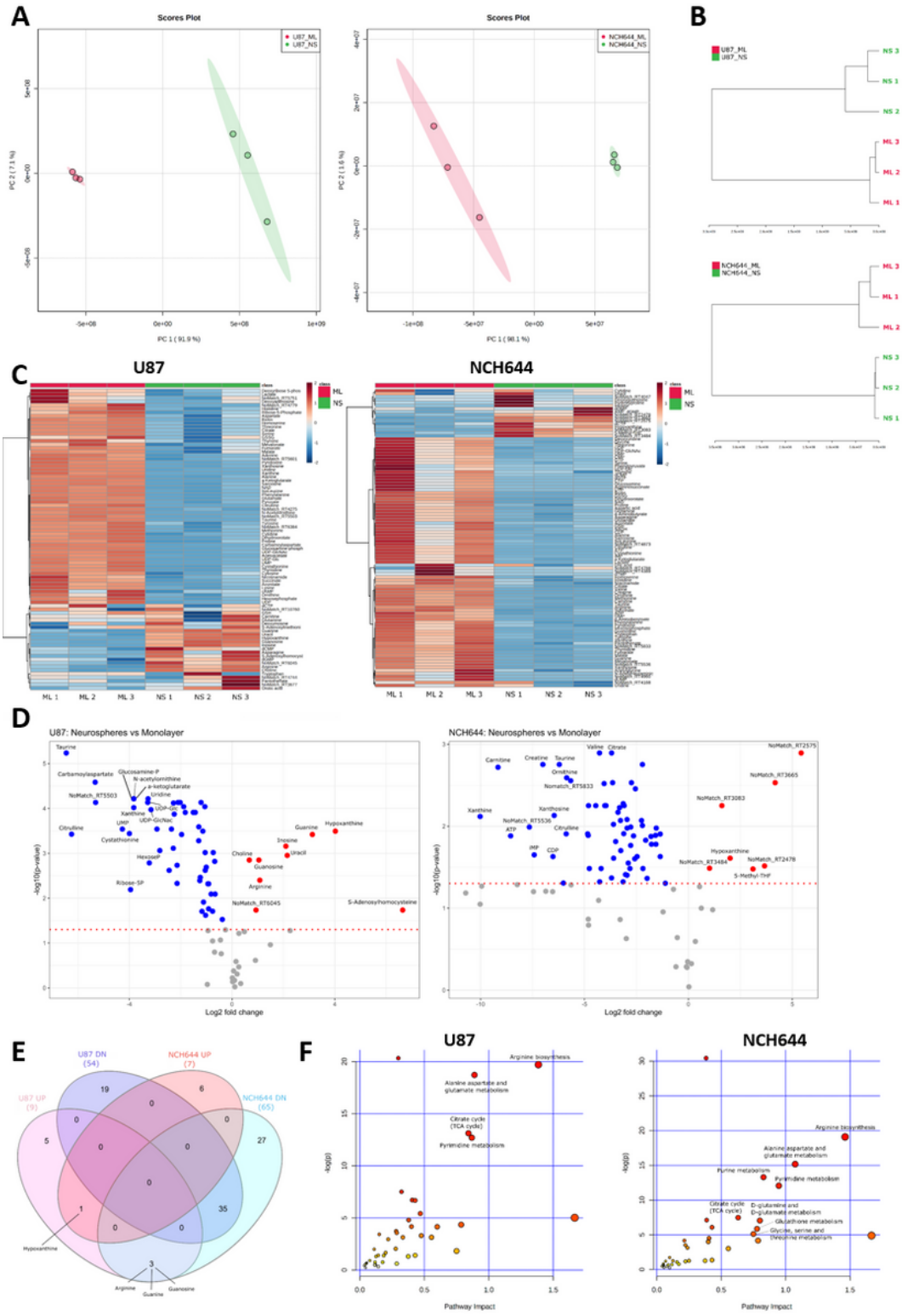

Figure 4

Metabolomics analysis of ML and NS from U87 and NCH644 cells. A) Principal component analysis and B) Hierarchical clustering off all metabolites, showing a clear separation between ML and NS samples in both cell lines. C) Heatmaps and D) Volcano plots of increased (red) and decreased (blue) metabolite levels in NS vs ML from U87 and NCH644 cells (FDR<0.05). E) Venn diagram depicting the number of significantly increased and decreased metabolites in NS vs ML, as well as commonly and differentially

regulated metabolites between U87 and NCH644 cells (FDR<0.05). F) Metaboanalyst analysis of significantly regulated metabolites in NS vs ML from U87 and NCH644 cells (FDR<0.05, Pathway impact>0.5). n=3

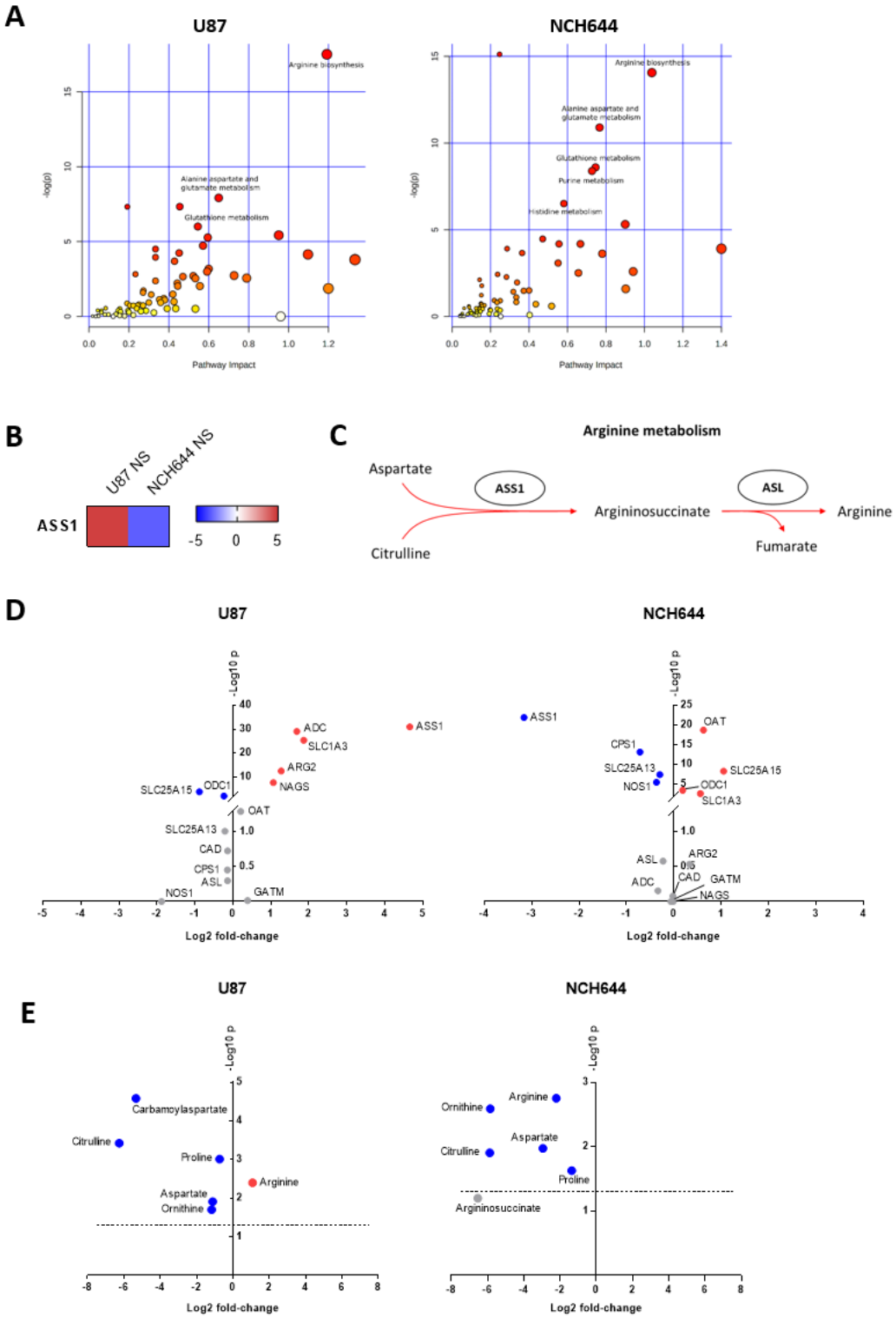

Figure 5

Joint pathway analysis of NS vs ML reveals arginine biosynthesis as the most significantly regulated pathway. A) Joint pathway analysis of significantly regulated metabolites (FDR<0.05) and genes

(FDR<0.05, log2FC>±1) in NS vs ML from U87 and NCH644 cells. B) ASS1 is significantly upregulated in U87 NS and downregulated in NCH644 NS, compared to ML cells (FDR<0.05). C) Schematic view of the arginine biosynthesis process. D) Significantly upregulated (red) and downregulated (blue) genes involved in arginine metabolism, in NS vs ML from U87 and NCH644 cells (FDR<0.05). E) Metabolites involved in arginine metabolism whose levels are significantly increased (red) and decreased (blue), in NS vs ML from U87 and NCH644 cells (FDR<0.05). n=3 ADC - arginine decarboxylase; ARG – arginase; ASL - argininosuccinate lyase; ASS1 - argininosuccinate synthase; CAD - carbamoyl-phosphate synthetase 2, aspartate transcarbamylase and dihydroorotase; CPS1 - carbamoyl-phosphate synthase 1; GATM - Glycine Amidinotransferase; NAGS - N-acetylglutamate synthase; NOS1 - nitric oxide synthase 1; OAT - ornithine aminotransferase; ODC1 - ornithine decarboxylase 1; SLC1A3 - solute carrier family 1 member 3; SLC25A13 - solute carrier family 25 member 13; SLC25A15 - solute carrier family 25 member 15

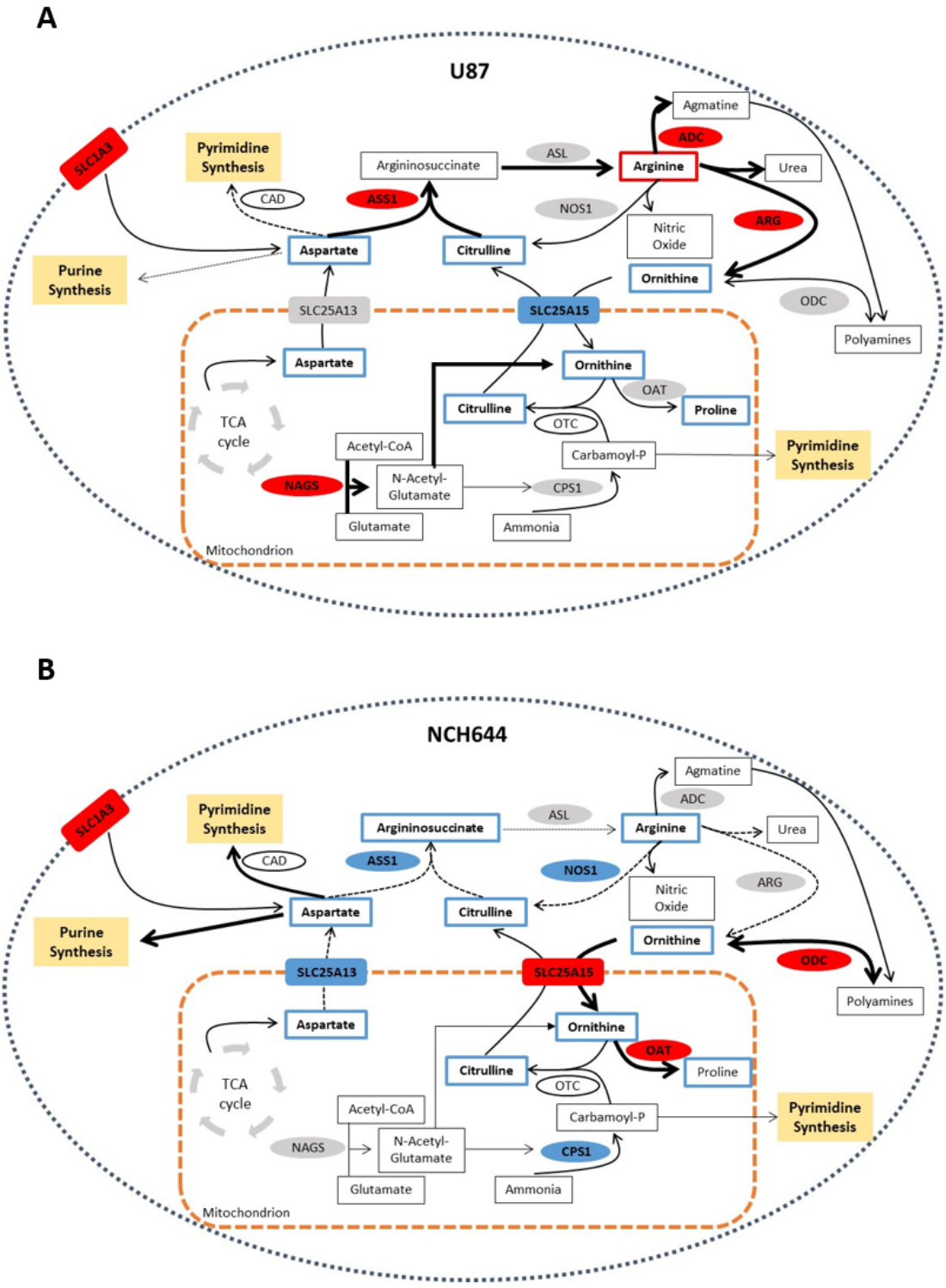

Figure 6

Proposed model of arginine metabolism in U87 and NCH644 NS. A) U87 NS present ASS1 upregulation, pointing towards aspartate shuttling into arginine synthesis. Arginine may be used by ADC or ARG in the cytoplasm for agmatine and ornithine production, respectively. By upregulating NAGS, ornithine production may be further induced to maintain a high flux of arginine synthesis. Increased arginine synthesis and urea cycle metabolism in these cells, may result in nucleotide metabolism reduction, by

pushing away aspartate pools from purine and pyrimidine synthesis. B) NCH644 NS, by downregulating ASS1, may shuttle aspartate away from arginine biosynthesis and towards nucleotide production. Ornithine may be used by ODC in the cytoplasm for polyamines production or translocate to the mitochondria through the SLC25A15 transporter to be used by OAT for proline synthesis. This way, these cells avoid feeding the urea cycle metabolism and may increase purine and pyrimidine synthesis to support their growth. ADC - arginine decarboxylase; ARG – arginase; ASL - argininosuccinate lyase; ASS1 - argininosuccinate synthase; CAD - carbamoyl-phosphate synthetase 2, aspartate transcarbamylase and dihydroorotase; CPS1 - carbamoyl-phosphate synthase 1; NAGS - N-acetylglutamate synthase; NOS1 - nitric oxide synthase 1; OAT - ornithine aminotransferase; ODC1 - ornithine decarboxylase 1; SLC1A3 - solute carrier family 1 member 3; SLC25A13 - solute carrier family 25 member 13; SLC25A15 - solute carrier family 25 member 15

Supplementary Files

This is a list of supplementary files associated with this preprint. Click to download.

- Additionalfile1.xlsx